CHEMICAL ENGINEERING TRANSACTIONS

VOL. 62, 2017

A publication of AIDIC

The Italian Association of Chemical Engineering
Online at www.aidic.it/cet

Guest Editors: Fei Song, Haibo Wang, Fang He

ISBN 978-88-95608- 60-0; **ISSN** 2283-9216

DOI: 10.3303/CET1762050

Oil Residual Layers in Water-Oil Displacement Flow

Jieheng Zheng, Weiming Zhang, Junze Jiang*, Jiang Li, Rui Guo

Department of Petroleum Supply, Army Logistics University of PLA, Chongqing 401331, China
327005868@qq.com

This paper investigates on the water-oil displacement flow in downward inclined pipe, which is a practical application in chemical and oil industry. The experiments were conducted in a 3.5m long 15mm inner diameter downward transparent pipe. The pipe can be flexibly tilted to specific inclination and water inlet velocity was controlled by a needle valve. During the experiments, it was revealed that in a certain range of pipe inclination and water inlet velocity, the oil layers remained stationary in the upper section of the pipe and it lasted through the entire displacement procedure. Meanwhile the thickness of the oil layers was altered according to different displacing configurations. A dimensionless parameter $\hat{\lambda}$ is introduced to represent the relative magnitudes of buoyancy stress and viscous shear stress. Based on the two-fluid model the relationship between normalized water-oil interface height and the dimensionless parameter is established. It is found that the transition from stable interface to unstable interface will be induced by the dominated inertia force or interface instability. Two critical value of the dimensionless parameter are derived as two criterions for the transition to from stable interface to unstable interface. The model prediction and criterions are in good agreement with the experiment results, thus verifying the effectiveness of the model.

1. Introduction

Water-oil displacement flow is a popular method for secondary oil recovery and pipeline pigging. By the method, water is injected to displace oil from reservoirs or pipelines. The displacement flow exhibits distinct flow patterns under different principal forces, such as buoyancy, inertia force and viscous force. According to previous miscible displacement experiments on downward pipes, the lighter displaced fluid may remain stationary in the upper section if the buoyancy and viscous force are balanced in the axial direction during water flooding (Taghavi et al., 2011). Because these experiments mainly tackle the near-horizontal miscible displacement flow of fluids with similar density and equal viscosity, the results on the stationary layers do not apply to the water-oil displacement flow with varied fluid viscosity and miscibility. The inapplicability, coupled with the yearn for efficient displacement, motivates the research into the transient flow regime of water-oil displacement.

Most of the previous studies have focused on immiscible displacement flows. If a less viscous fluid is displaced by a more viscous one, the displaced fluid often penetrates into the displacing fluid, forming a two or three-layer flow structure (Sahu et al., 2009). Through analytical and numerical explorations, it is proved that the static wall layers of yield stress fluids are likely to stick on the pipe wall (Frigaard et al., 2007; Redapangu et al., 2012). In contrast, the immiscible displacement flows have almost no diffusion effect between phases, and the different interfacial tensions, diffusions and viscosity ratios of the displacement flows help to stabilize the interfaces (Selvam et al., 2007).

For water-oil displacement flow, the research interests are concentrated in flow pattern, pressure drop, water holdup, and residual layer properties. For example, the two-fluid model was successfully employed to predict the pressure gradient and water holdup of stratified water-oil flow, but was proved as ineffective in some horizontal systems. The two-fluid model was later modified and adapted to several different flow configurations, such as the modified two-fluid model for curved interface (Edomwonyi-Otu and Angeli, 2015), and the CA model for core-annular flow (Asiegubu and Asakura, 2008; Beretta et al., 1997; Brauner, 1991). When it comes to the displacement flows in stationary regimes, the interface profile was often simulated by the lubrication model based on momentum balance (Séon et al., 2007).

To sum up, despite the in-depth discussion of immiscible displacement flows, there is only limited research into stationary residual layers, a determinant of displacement efficiency, and the transient state in Newtonian immiscible displacement flows. In light of the problem, this paper probes into the stationary residual oil layers in water-oil displacements. First, several experiments were performed to explain the phenomenon of the stationary oil layers. Then, the interface height model was derived, together with the interface transition criterion. Finally, the experimental results were analyzed and compared with model predictions.

2. Experimental system and procedure

According to the pipeline system loop in Figure 1, the displacement was conducted in a 3.5m-long downward glass pipe (ID: 15mm). The pipe was connected to a hose at either end and fixed on a tillable steel frame. The pressure was supplied by a pressure water tank, designed to offset the mechanical vibration of the water pump and supply a relative stable inlet flow. To distinguish the water and oil phases and visualize the oil-water interface, fluorescence yellow coloring agent only dissolvable in oil was added to diesel. The physical properties of the dyed diesel are listed in Table 1.
At the beginning of the experiments, a high-speed diesel oil flow was pumped from the oil tank to displace the air and water in the glass pipe. Once the diesel oil reached steady state, water was injected into the glass pipe as the displacing fluid. The water flow rate was adjusted by a needle valve. The valve opening was set prior to water injection and remained constant throughout the displacement. The water injection continued until the flow arrived at a steady state. The surface water flow rate was measured by two rotameters (accuracy: 2%) with different measuring ranges in the upstream of the glass pipe. The entire displacement process was recorded by a digital camera at 800fps.
The purpose of the experiments is to figure out the relationship between the interface height of stationary residual layers and other factors (e.g. inlet water velocity or pipe tilt angle). The inlet water velocity varied from 8mm/s to 220mm/s, and the pipe tilt angle ranged from 5° to 30°. Each inlet water velocity and pipe tilt angle were tested in the experiments, to ensure the stability and estimate the errors of the results. Based on the images captured in the experiments, the author obtained the concentration distribution of oil phase and water phase and deduced the interface height.

Table 1: Properties of experimental fluids at 21° C

	Water	Diesel
Density (kg/m^3)	998.3	829.4
Viscosity (mPa s)	1.0	3.3
Diesel – water interfacial tension (mN/m)	18.2	

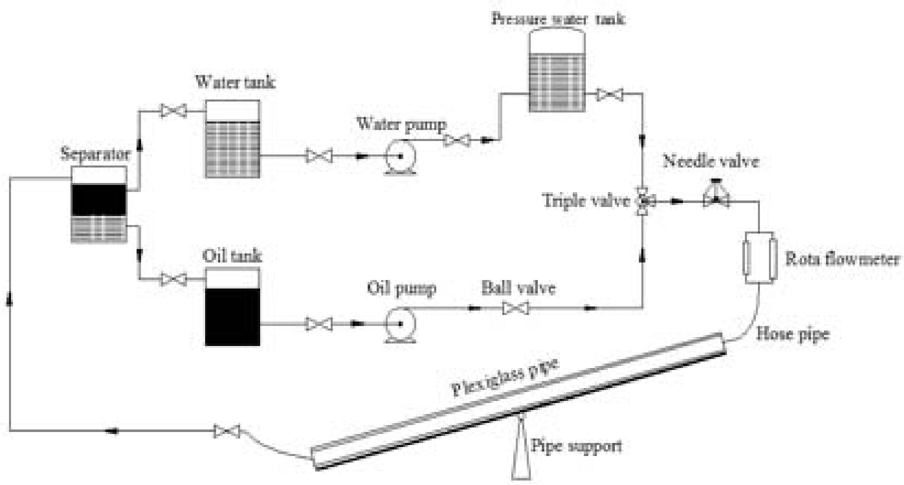

Figure 1: Schematic view of experimental setup

3. Experimental observations

Figure 2 presents the steady-state images of the displacement flow under different water inlet velocities V_0 (20mm/s~60mm/s) and the same pipe tilt angle (5°). It is observed that the upper oil layers remained stationary throughout the displacement, while the water kept flowing through the lower pipe section with a smooth interface. As shown in Figures 2(a)-2(d), it is crystal clear that the interface height is negatively correlated with V_0 in a certain range, there was always an interface height corresponding to each specific V_0. With further increase in water inlet velocity, the oil was pushed downstream and completely displaced by water flooding. In the meantime, stationary oil layers disappeared as the experiments proceeded, as shown in Figure 2(e). This implies the existence of stationary threshold for the oil layers in the upper pipe section.

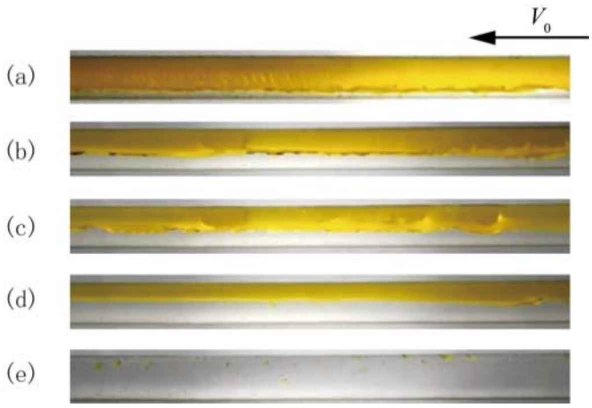

Figure 2: Stationary residual oil layers at the pipe tilt angle of 5° and the inlet water velocities of (a)10.43mm/s, (b)26.72mm/s, (c)36.15mm/s, (d)58.16mm/s and (e)63.82mm/s. The water inlet is located at the right end of the pipe.

According to the observed oil-water interfaces in Figure 3, the displacement flows were classified into 3 types. The smooth interface mainly appeared at a low inlet water velocity and a small pipe tile angle. It is featured by a flat interface along the length of the pipe. The interface turned waxy with the increase in inlet water velocity and pipe tile angle. In the regimes of smooth and waxy interfaces, the velocity of oil phase remained attached to the pipe wall. The unstable interface refers to the regime for which the oil layers were destabilized, scattered and washed away during the experiments. As no steady oil layers formed in this regime, the images captured for this type of interface were in transient state. Both plug flow and dispersed flow were observed in this regime.

Type of interface	Images
Smooth interface	
Waxy interface	
Unstable interface (transient)	

Figure 3: Types and images of oil-water interface

4. Model for the interface height

According to the experiments, the stationary oil phase was separated from the moving water phase by a smooth or waxy interface. The zero velocity of the oil phase can be considered as a special case of stratified oil-water flow. Here, a dimensionless variable $\hat{h} = h/d$ and a dimensionless parameter $\hat{\lambda}$ are introduced to respectively represent the relative magnitudes of buoyancy and viscous force along the z axis:

$$\hat{\lambda} = \frac{2\Delta\rho g d \sin\alpha}{f_w \rho_w V_0^2} \tag{1}$$

Where *w*, *o* and *i* refer to water phase, oil phase and interface, respectively; *d* is the hydraulic diameter; *A* and *ρ* are the area and density of the two phases, respectively; $\Delta\rho = \rho_w - \rho_o$; *g* is the gravitational acceleration; *α* is pipe tilt angle; *f* is the friction factor. The numerator equals the buoyancy, and the denominator equals the viscous force.
Assuming that the displacement flow was fully developed and reached the steady state with no dispersion at the interface, the one-dimensional two-fluid model based on momentum balance is suitable for calculating the interface height (Rodriguez and Castro, 2014). With the two dimensionless parameters $\hat{h}$ and $\hat{\lambda}$, the two-fluid model can be transformed into a dimensionless format:

$$\hat{\lambda} = \varphi\left(\hat{h}\right) = \frac{4A^2}{A_w^2}\left[\frac{\left(\pi - C_g\right)\arccos\left(1-2\hat{h}\right) + C_{iw}\pi\sqrt{1-\left(1-2\hat{h}\right)^2}}{C_g\left(\pi - C_g\right)}\right] \tag{2}$$

in which

$$C_g = \arccos\left(1-2\hat{h}\right) + \left(2\hat{h}-1\right)\sqrt{1-\left(1-2\hat{h}\right)^2} \tag{3}$$

$$C_{iw} = \frac{f_i}{f_w} = \left(1 + C_i\frac{\varepsilon}{d}\right)\left(\frac{\pi D_w}{S_i}\right)^n \tag{4}$$

where *U* is the phase velocity; *m* and *n* are 0.046 and 0.2 for turbulent flow, and 16 and 1 for laminar flow, respectively; C_i is the interfacial roughness correction coefficient valued as 50 (Rodriguez and Baldani, 2012); *ε* is the interface wave amplitude. For smooth interface, the interface wave amplitude is so small as to be negligible. For waxy interface, the average measured interface wave amplitude is 0.0004m±0.0002m.
Hence, the dimensionless interface height $\hat{h}$ is correlated with the dimensionless parameter $\hat{\lambda}$. The extreme point is located at $\hat{\lambda} \geq \hat{\lambda}_{cr} = 36.71$ and $\hat{h} \leq \hat{h}_{cr} = 0.68$`. If $\hat{h} > 0.68$`, the principle force is the inertia force, which destabilizes the layer and leads to instantaneous displacement. The interface height also depends on the interface slope, because the later affects the pressure gradient along the length of pipe. However, the interface slope is basically zero at the steady state. In the long run, the interface height is solely determined by the parameter $\hat{\lambda}$.

5. Results and discussion

Figure 5 illustrates the experimental results corresponding to the changing parameters. In the figure, the x-axis is the viscous force and the y-axis is the buoyancy; the black solid line represents the interface instability threshold $\hat{\lambda} = \hat{\lambda}_{cr}$ derived from equation (2); the yellow solid line represents the interface instability threshold $\hat{\lambda} = \hat{\lambda}_{KH}$ (Torres et al., 2015). It can be seen that the flow regime separation criterion agrees well with the experimental results. It is possible to identify three flow regimes from the figure:

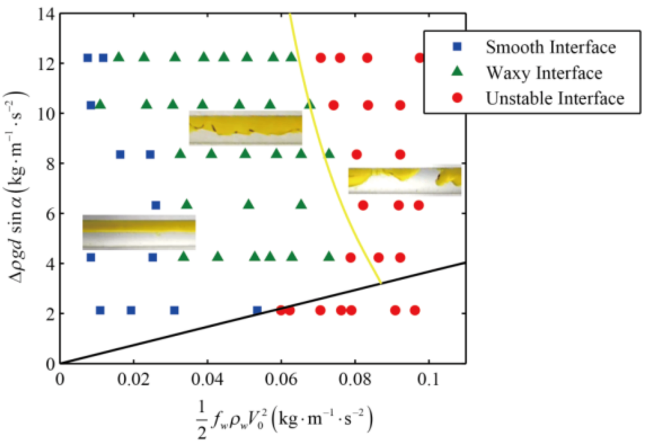

Figure 5: Experimental results corresponding to the changing parameters

Regime a: $\hat{\lambda} \le \hat{\lambda}_{\mathrm{cr}}$. In this regime, the dominance of inertia force and viscous over buoyancy destabilizes the oil layer and induces instantaneous displacement.

Regime b: $\hat{\lambda} > \hat{\lambda}_{\mathrm{cr}}$ and $\hat{\lambda} < \hat{\lambda}_{\mathrm{KH}}$. In this regime, the buoyancy inertia force and viscous force are balanced along the x-axis. However, the interface instability may lead to flow pattern transition and breakage of the oil layer.

Regime c: $\hat{\lambda} > \hat{\lambda}_{\mathrm{cr}}$ and $\hat{\lambda} \ge \hat{\lambda}_{\mathrm{KH}}$. In this regime, the interface is stable and the buoyancy is offset by inertia force and viscous force. Thus, the oil layer remains stationary in the upper section of the pipe.

It is reasonably to conclude that the parameter $\hat{\lambda}_{\mathrm{cr}}$ can serve as a conservative criterion for the emergence of stationary oil layer in industrial applications.

Figure 6 shows the variation in dimensionless interface height $\hat{h}$ with the dimensionless parameter $\hat{\lambda}$ based on the experimental data and predicted data. The comparison shows a good agreement between our model and the experiments on smooth interface, and relatively large deviation between the two on waxy interface.

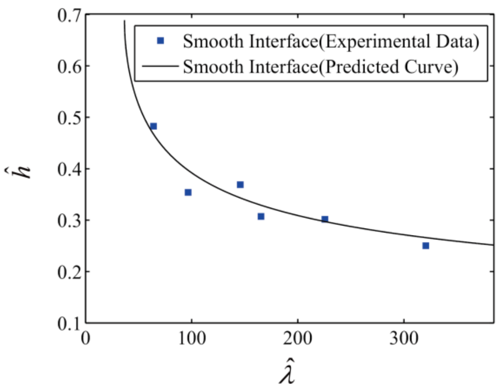

(a) α=5°

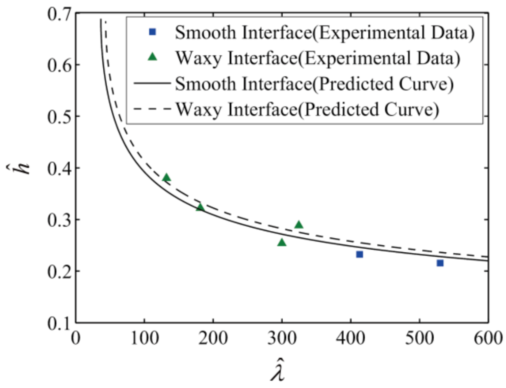

(b) α=15°

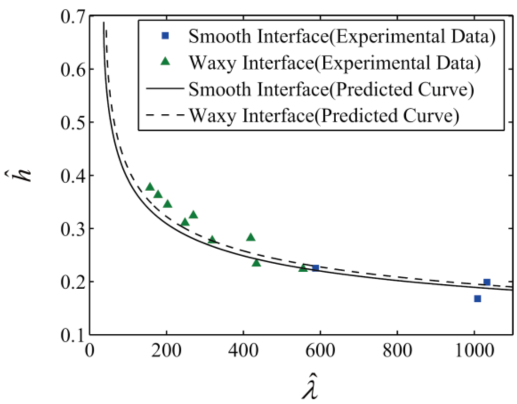

(c) α=20°

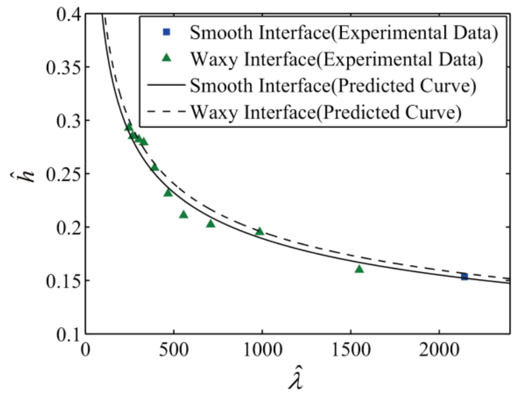

(d) α=25°

Figure 6: Comparison of predicted and experimental interface heights at different pipe tilt angles

6. Conclusions

This paper explores the phenomenon of stationary residual oil layers in water-oil displacement flows. Unlike the wax formation in the displacement of waxy crude oil, the stationary residual oil layers of Newtonian water-oil displacement are resulted from the balance between buoyancy and viscous force in the flows along the length of the pipe.

According to the steady-state interfaces of the flows, the flow patterns were classified into such 3 categories as smooth interface, waxy interface and unstable interface. The height and shape of the interface were adjusted by the flow configuration. Then, a dimensionless parameter was introduced to represent the relative

magnitudes of buoyancy and viscous force. The relationship of the interface height and the dimensionless parameter was established based on the one-dimensional two-fluid model.
Through comparison, the author discovered a good agreement between model predictions and the experiments on smooth interface, and relatively large deviation between the two on waxy interface. To further improve the accuracy, more variables will be introduced based on the complex displacement configuration in actual operations of the oil industry.

Acknowledgments

We thank the Department of Oil Supply Engineering for the support in the experimental design and setup.

Reference

Asiegubu C.P., Asakura K., 2008, Experimental Study on Pressure Loss of Horizontal Core-Annular Flow, Journal of Solid Mechanics and Materials Engineering, 2, 831-841, DOI: 10.1299/jmmp.2.831
Beretta A., Ferrari P., Galbiati L., Andreini P.A., 1997, Horizontal oil-water flow in small diameter tubes, Flow patterns, International Communications in Heat & Mass Transfer, 24, 223-229.
Brauner N., 1991, Two-phase liquid-liquid annular flow, International Journal of Multiphase Flow, 17, 59-76.
Edomwonyi-Otu L.C., Angeli P., 2015, Pressure drop and holdup predictions in horizontal oil–water flows for curved and wavy interfaces, Chemical Engineering Research and Design, 93, 55-65, DOI: 10.1016/j.cherd.2014.06.009
Frigaard I., Vinay G., Wachs A., 2007, Compressible displacement of waxy crude oils in long pipeline startup flows, Journal of Non-Newtonian Fluid Mechanics, 147, 45-64, DOI: 10.1016/j.jnnfm.2007.07.002
Redapangu P.R., Chandra Sahu K., Vanka S.P., 2012, A study of pressure-driven displacement flow of two immiscible liquids using a multiphase lattice Boltzmann approach, Physics of Fluids, 24, 102-110, DOI: 10.1063/1.4760257
Rodriguez O. M. H., Baldani L.S., 2012, Prediction of pressure gradient and holdup in wavy stratified liquid–liquid inclined pipe flow, Journal of Petroleum Science and Engineering, 96-97, 140-151, DOI: 10.1016/j.petrol.2012.09.007
Rodriguez O.M.H., Castro M.S., 2014, Interfacial-tension-force model for the wavy-stratified liquid–liquid flow pattern transition, International Journal of Multiphase Flow, 58, 114-126, DOI: 10.1016/j.ijmultiphaseflow.2013.09.003
Séon T., Znaien J., Salin D., Hulin J.P., Hinch E.J., Perrin B., 2007, Transient buoyancy-driven front dynamics in nearly horizontal tubes, Physics of Fluids, 19, 123603, DOI: 10.1063/1.2813581
Sahu K.C., Ding H., Valluri P., Matar O.K., 2009, Linear stability analysis and numerical simulation of miscible two-layer channel flow, Physics of Fluids, 21, 042-104, DOI: 10.1063/1.3116285
Selvam B., Merk S., Govindarajan R., Meiburg E., 2007, Stability of miscible core–annular flows with viscosity stratification, Journal of Fluid Mechanics, 592, DOI: 10.1017/s0022112007008269
Taghavi S.M., Séon T., Wielage-Burchard K., Martinez D.M., Frigaard I.A., 2011, Stationary residual layers in buoyant Newtonian displacement flows, Physics of Fluids, 23, 044-105, DOI: 10.1063/1.3581063
Torres C.F., Mohan R.S., Gomez L.E., Shoham O., 2015, Oil–Water Flow Pattern Transition Prediction in Horizontal Pipes, Journal of Energy Resources Technology, 138, 022904, DOI: 10.1115/1.4031608